



Regioselectivity and memory effects in palladium catalyzed allylic alkylations with bidentate $P^{\wedge}P=S$ donor ligands

Suzanna C. Milheiro¹, J.W. Faller*

Yale University, P.O. Box 208107, New Haven, CT 06520-8107, United States

ARTICLE INFO

Article history:

Received 10 August 2010

Received in revised form

6 October 2010

Accepted 8 October 2010

Available online 20 October 2010

Keywords:

Allylic alkylation

Memory effect

Catalysis

Rearrangements

Isomerization

Hemilabile

Regioselectivity

Conformational equilibria

Heterobidentate ligands

ABSTRACT

A series of complexes, $[Pd(\eta^3-C_3H_5)(P^{\wedge}P=S)][SbF_6]$, where $P^{\wedge}P=S$ are bidentate bisphosphine monosulfide ligands, were found to catalyze allylic alkylation reactions with high branched:linear selectivity with some ligands. Some of these catalysts also display a regiochemical memory effect, in which the hemilability and rigidity of the $P^{\wedge}P=S$ ligands affect the reaction rate and the degree to which a memory effect is observed.

© 2010 Elsevier B.V. All rights reserved.

1. Introduction

The design of ligands for asymmetric transition metal catalyzed reactions continues to grow in importance in synthetic chemistry [1]. Although great strides have been made in preparing ligands with the appropriate electronic and steric properties to impart high activity and selectivity to catalysts, it is often difficult to predict the properties that a metal complex of a given ligand will exhibit. Some parameters, however, can offer some predictive capabilities. The bite angle of bisphosphine ligands is known to influence the selectivity of transition metal catalyzed reactions [2,3]. This is usually attributed to a steric effect where a larger bite angle ligand has increased interactions with a substrate bound to the same metal center allowing more efficient transfer of chiral or other steric information [4]. This is particularly useful in palladium-catalyzed allylic addition reactions [5,6] where the regio- or enantio-determining steps occur on the side of the substrate remote from the asymmetric ligand. The rigidity of a ligand backbone further influences the rate and selectivity of asymmetric reactions [2].

The donor atoms of ligands also have a significant influence on transition metal catalyzed reactions and the use of ligands containing different donors has proven successful for some asymmetric reactions [7,8] including allylic substitution [9–11]. Heterobidentate ligands containing two different donors, often one hard and one soft donor, offer several advantages over traditional symmetrical bisphosphine ligands by creating steric and electronic asymmetry at the metal center [12], as well as opening the possibility for fluxional processes that may enhance the rate and selectivity of catalytic reactions. Another potential consequence of having donors with different properties is hemilability [13,14] where one donor is substitutionally inert and remains attached to the metal center while the other donor is labile. During a catalytic cycle, dissociation of the more labile donor can create an open site for substrate binding, while re-coordination of that donor can temporarily stabilize a potentially coordinatively unsaturated metal center at another step in the catalytic process.

Hemilability has further applications in asymmetric catalysis where hemilabile ligands may allow interconversion of diastereomeric isomers to form a preferred isomer that could then serve as an asymmetric catalyst. Previously [15], we studied hemilability and nonrigidity in a series of rhodium and palladium complexes of $P^{\wedge}P=S$ donor ligands using variable temperature 1H , ^{13}C , and ^{31}P NMR. We determined the barrier to hemilability was lowest for $P^{\wedge}P=S$ donor ligands forming larger chelate rings. The rigidity of

* Corresponding author. Fax: +1 203 432 6144.

E-mail address: jack.faller@yale.edu (J.W. Faller).

¹ Present address: Western New England College, 1215 Wilbraham Road, Springfield, MA 01119, United States.

the ligand backbones and η^3 -allyl fluxional processes were also examined. The present study aims to increase understanding of the regioselectivity and memory effects observed in Pd-catalyzed allylic alkylations with respect to the donor properties, hemilability, and nonrigidity of the $P^{\wedge}P=S$ ligands.

When butenyl substrates are used for allylic nucleophilic addition reactions, addition can occur at the terminal or internal position resulting in linear or branched products respectively. Palladium complexes of chiral $P^{\wedge}P=S$ ligands are known to be selective for branched products in enantioselective nucleophilic addition reactions to allylic substrates [10,11]. It is proposed that this is the result of the steric and electronic asymmetry of $P^{\wedge}P=S$ ligands. The allyl substrate prefers to bind in an η^3 fashion to palladium with its substituted terminus *trans* to the bulky PPh_2 group and *cis* to the smaller $Ph_2P=S$ group. The nucleophile then attacks the allyl substrate *trans* to the more π -accepting P(III) donor resulting in a preference for the branched product. This selectivity is in contrast to palladium bisphosphine catalysts which generally lead to addition at the less-hindered allyl terminus and are considered complementary to tungsten [16] and molybdenum [17,18] systems which lead to addition at the more hindered terminus [19]. Rhodium [20–23] and iridium [24–28] systems have also been shown to catalyze nucleophilic addition to the more substituted allylic terminus.

The branched product may result in the formation of a stereocenter and a number of chiral catalysts that are selective for the branched product are enantioselective. Although a number of studies have been reported on the regioselectivity of allylic addition reactions based on bite angle [4] and donor effects [29] for palladium systems giving primarily linear product, high branched selectivity from palladium catalysts is far less common [10,11,30] and few studies have addressed this type of regioselectivity. Formation of branched products is potentially more important because a chiral center could be generated enantioselectively when addition occurs to the substituted terminus of an unsymmetrically substituted allyl fragment. The relationship between bidentate ligand bite angle and regioselectivity has been explored for bisphosphine ligands [4] and analogous ligands with different donors [31] including heterobidentate ligands. These complexes generally give a preference for linear product despite differences in branched:linear ratios that may be tuned through ligand bite angle and choice of donor. A few catalysts have been shown to reverse the normal selectivity of palladium to give primarily branched product, yet these studies have been mainly with chiral catalysts and focus on enantioselectivity [11,32–34]. There are fewer studies focusing on regioselectivity with achiral ligands [31].

We have shown that achiral $P^{\wedge}P=S$ ligands are effective for palladium-catalyzed regioselective nucleophilic addition to allylic carbonates and have studied this selectivity in the absence of chiral modifiers. Unlike their $P^{\wedge}P$ donor analogues, $P^{\wedge}P=S$ donor ligands favor branched product formation. Yet, similarly to the bisphosphine ligands, larger bite angle $P^{\wedge}P=S$ ligands further increase selectivity for the branched product. The relative rates of allyl rearrangement, hemilability and nucleophilic attack also influence the branched:linear product ratio. The $[Pd(\eta^3-C_3H_5)(P^{\wedge}P=S)][SbF_6]$ (**1**) complexes studied were found to be active catalysts for allylic alkylation reactions, and the regioselectivity can be tuned by varying the bite angle of the $P^{\wedge}P=S$ ligand. These catalysts also display a regiochemical memory effect, and the hemilability and rigidity of the $P^{\wedge}P=S$ ligands affect the reaction rate and the degree to which a memory effect is observed.

2. Results and discussion

2.1. $[Pd(\eta^3-C_3H_5)(P^{\wedge}P=S)][SbF_6]$ (**1a–i**) catalyzed allylic alkylation

A series of complexes $[Pd(\eta^3-C_3H_5)(P^{\wedge}P=S)][SbF_6]$ (**1a–i**) were prepared. Observations of changes in the fluxional processes

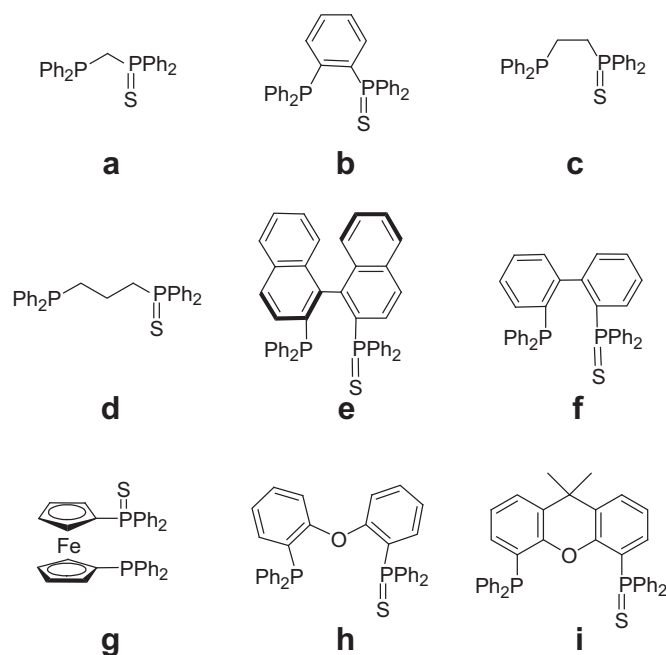
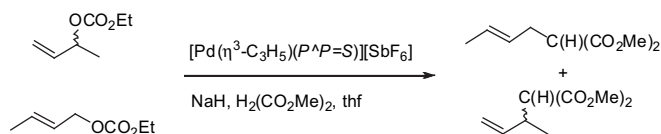


Fig. 1. Bisphosphine monosulfide ligands in **1**.

resulting from differences in ligand bite angle and backbone rigidity have been reported [15] for some of these complexes. The $P^{\wedge}P=S$ ligands were all bisdiphenylphosphine monosulfides as shown in Fig. 1.

The $P^{\wedge}P=S$ complexes of palladium (**1**) were tested as catalysts for the alkylation of allylic carbonates (Scheme 1) in order to assess the effect of bite angle, hemilability and ligand rigidity on the regioselectivity. The reactions of sodium dimethyl malonate and either the crotyl carbonate or the 3-buten-2-yl carbonate were catalyzed with the appropriate complex at 2.5% loading and allowed to proceed at 20 °C or –20 °C. The ratio of branched to linear products was determined by 1H NMR in each case. A comparison of the results for the linear and the branched substrate is presented in Table 1.

Three notable features were observed in comparison of results for the regioselectivity of the alkylation of crotyl (Table 1) and 3-buten-2-yl (Table 1) carbonates with sodium dimethyl malonate catalyzed by **1**. (1) Relative to palladium complexes incorporating bisphosphine ligands, the use of $P^{\wedge}P=S$ donor ligands generally reversed the selectivity from a preference for linear product to a preference for branched product, particularly when the branched substrate was used. It was only when the linear substrate was used that a significant preference for the linear product was observed. (2) An increase in the chelate ring size of the $P^{\wedge}P=S$ ligand increased the preference for branched product, with the only exceptions to this trend being those ligands displaying a memory effect. (3) A memory effect was observed with several of the $P^{\wedge}P=S$ ligands so that with a given ligand the branched product was produced in relatively higher amount when the branched substrate was used than when the linear substrate was used.



Scheme 1. Allylic alkylation of butenyl carbonates.

Table 1
Allylic alkylation catalyzed by **1a–i**.

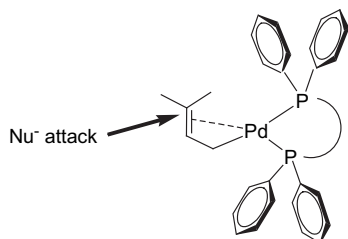
Substrate ($P^{\wedge}P=S$)	Crotyl carbonate				3-Buten-2-yl carbonate			
	20 °C		–20 °C		20 °C		–20 °C	
	Conversion % ^a	B:L	Conversion % ^b	B:L	Conversion % ^a	B:L	Conversion % ^b	B:L
Ph ₂ P(S)CH ₂ PPh ₂ (a)	100	50:50	100 ^c	50:50	100	50:50	100 ^c	50:50
Ph ₂ P(S)(CH ₂) ₂ PPh ₂ (c)	100	65:35	100	70:30	100	66:34	100	70:30
Ph ₂ P(S)(CH ₂) ₃ PPh ₂ (d)	85	63:37	100	57:43	100	64:36	100	62:38
Ph ₂ P(S)(<i>o</i> -C ₆ H ₄)PPh ₂ (b)	82	53:47	21	56:44	61	58:42	92	70:30
(<i>S</i>)-BINAP(S) (e)	97	50:50	100	47:53	100	73:27	100	79:21
Biphep(S) (f)	100	39:61	100	31:69	100	81:19	100	77:23
Dppf(S) (g)	100	63:37	100	67:33	100	78:22	100	83:17
DPEphos(S) (h)	98	75:25	100	85:15	100	75:25	100	85:15
Xantphos(S) (i)	100	76:24	100	80:20	100	76:24	100	80:20

^a After 1 h.^b After 20 h.^c Reaction was complete after 1 h.

2.2. Effect of $P^{\wedge}P=S$ donor

We have observed a strong preference for branched product with most $P^{\wedge}P=S$ donor ligands and no ligand giving more than 69% linear product (**1f**) with the linear substrate or 50% linear product (**1a**) with the branched substrate. The nature of the $P^{\wedge}P=S$ donor ligands is significantly different from that of the $P^{\wedge}P$ donor ligands and can be considered to be responsible for the reversal of the normal selectivity. The rate of addition to the substituted terminus relative to the unsubstituted terminus of an allyl fragment is a balance between steric and electronic properties of the system [19,29,35,36]. In the case of the $P^{\wedge}P=S$ donor ligands, the steric asymmetry primarily dictates the orientation of the substrate, while the electronic asymmetry directs nucleophilic attack. It is known [36] that for the cationic complexes [Pd(1,1-dimethylallyl)]($P^{\wedge}P$)⁺ there is a distortion of the allyl ligand bonding to palladium (Fig. 2). Interaction of the phenyl groups with the allyl ligand causes a shift from an η^3 toward an η^1, η^2 bonding mode where the η^1 bound carbon is the unsubstituted carbon. This causes a shortening of the η^1 Pd–C bond and a lengthening of the Pd–C bonds involved in the η^2 bond relative to the η^3 bond of a symmetrical allyl ligand. Further it has been observed that the Pd–P bond *trans* to the η^1 bond will be lengthened while that *trans* to the η^2 bond will be shortened. This places the methyl substituents on the allyl in the less sterically hindered position. In the case of the $P^{\wedge}P=S$ ligands (Fig. 3), the sulfide acts as a spacer distancing the phenyl groups of one phosphorus from the allyl ligand. Therefore, we can expect the crotyl ligand to coordinate with a strong thermodynamic preference for the methyl group disposed *cis* to the sulfide.

We can further compare the $P^{\wedge}P=S$ ligands to the $P^{\wedge}P$ case electronically. In the $P^{\wedge}P$ complexes, there is greater donation and back donation in the shorter Pd–P bond than in the longer Pd–P bond. There will be less back donation to the η^2 bond than to the η^1 bond making the substituted terminal allyl position more electrophilic than the unsubstituted terminal allyl position [29]. Similarly, the symmetrically substituted 1,3-diphenyl allyl forms a distorted

Fig. 2. Allyl distortion in [Pd(1,1-dimethylallyl)]($P^{\wedge}P$)⁺.

η^3 -allyl complex induced by heterodonor phosphinooxazoline ligands. With these complexes, nucleophilic attack was shown to occur *trans* to the phosphorus donor [9]. In the same way, the weaker back donation to the sulfide will decrease the electrophilicity of the unsubstituted carbon *trans* to sulfur, and the stronger back donation to phosphorus will increase the electrophilicity of the substituted allyl carbon *trans* to phosphorus. This will activate the substituted carbon toward nucleophilic attack.

The distortion of an allylic substrate can be probed with ¹³C NMR. It has been shown that acceptor ligands increase the preference for nucleophilic attack at the more substituted terminus [29,31,35]. It has also been shown that the rate and regioselectivity of alkylation reactions correlate well to ¹³C NMR shifts of allylic termini [29]. It is therefore thought that these shifts can be used to compare acceptor properties of ligands. In the case of the $P^{\wedge}P=S$ donor ligands, the more accepting phosphine may induce a greater positive charge on the *trans* terminus relative to the *cis* terminus. This can be observed by ¹³C NMR where the substituted allylic terminus is shifted further downfield than the terminus *cis* to phosphorus. There is little variation in these chemical shifts for different $P^{\wedge}P=S$ ligands. The chemical shifts for the allylic terminus *trans* to P(III) ranges from δ 80.3–80.0 and the *cis* to P(III) allylic terminus chemical shifts range from δ 66.2–64.7 in **1c**, **1d**, and **1i**. These ¹³C NMR data support the premise that the $P^{\wedge}P=S$ donors help to create the desired electronic asymmetry in the allyl fragment, although the small range of chemical shifts does not allow us to predict which $P^{\wedge}P=S$ ligands will be most effective for inducing the distortion.

2.3. Effect of bite angle

We have discussed the difficulty in predicting the bite angles of complexes of $P^{\wedge}P=S$ donor ligands in a previous report [15]. Although, average bite angles for $P^{\wedge}P$ ligands have been reported [37], $P^{\wedge}P=S$ ligands do not necessarily follow the same trend as $P^{\wedge}P$ ligands. In some cases the sulfide donor causes an increase in bite

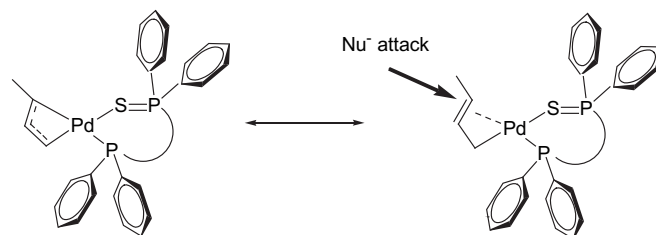
Fig. 3. Allyl distortion with $P^{\wedge}P=S$ donor ligands.

Table 2
Reported bite angles for $P^{\wedge}P$ and $P^{\wedge}P=S$ ligands.

$P^{\wedge}P$	β_{ave}^a	$Pd/P^{\wedge}P=S$	$Rh/P^{\wedge}P=S$	$M/P^{\wedge}P=S$
		β	β	β
$Ph_2PCH_2PPh_2$	71.53	95.74 ^b 91.21 ^c	89.3 ^d	
$Ph_2P(o-C_6H_4)PPh_2$	81.95			86.4 ^f
$Ph_2P(CH_2)_2PPh_2$	82.55	90.17 ^e		
$Ph_2P(CH_2)_3PPh_2$	91.56			
Biphep	91.63 ^g	92.85 ^h		
(S)-BINAP	92.77	92.83 ⁱ 89.11 ^j 99.01 ^k 100.45 ^l		
Dppf	98.74			85.75 ^m
DPEphos	101.46	99.2 ⁿ		
Xantphos	104.64	102.61 ^o	93.0 ^p	

^a Average bite angles from the Cambridge Crystallographic Database [37].

^b $[Pd(\eta^3-C_3H_5)-(dppm(S))][Otf]$ [38].

^c $[Pd(II)(dppm(S))_2]$ [39].

^d $[RhCOD(dppm(S))][SbF_6]$ [15].

^e $[Pd(diphos(S)Cl_2)]$ [40].

^f $[Ru(\eta^6:\eta^1-NMe_2-C_6H_4-C_6H_4PCy_2)(diphos(S))][SbF_6]$ [41].

^g $[Rh(2-(4-tert-butyl-phenyl)-8-methoxy-1,8-dimethyl-bicyclo-[2.2.2]octa-2,5-diene)(biphep)][SbF_6]$ [42].

^h $[Pd(\eta^3-C_3H_5)(biphep(S))][SbF_6]$ [11].

ⁱ $[Pd(\eta^3-C_3H_5)((S)-BINAP(S))][BF_4]$ [43].

^j $[Pd((S)-BINAP(S)Cl_2)]$ [43].

^k $[Pd(\eta^3-cinnamylallyl)((S)-BINAP(S))][SbF_6]$ [11].

^l $[Pd-(\eta^3-1,1-dimethylallyl)((S)-BINAP(S))][SbF_6]$ [11].

^m $[Pd(Me_8-dppf(S)Cl_2)]$ [44].

ⁿ $[Pd(\eta^3-C_3H_5)(DPEphos(S))][SbF_6]$.

^o $[Pd(\eta^3-C_3H_5)(xantphos(S))][SbF_6]$.

^p $[RhCOD(xantphos(S))][SbF_6]$ [15].

angle while other ligands show contracted bite angles with the sulfide donor relative to the parent $P^{\wedge}P$ donor ligand. The bite angles of known $P^{\wedge}P=S$ complexes are presented in Table 2 in order to illustrate the large variation in bite angle that is possible for a given $P^{\wedge}P=S$ ligand. This variation is illustrated in the bite angles observed for (S)-BINAP(S) found in various complexes ranging from 89.11° to 100.45° while the parent bisphosphine has a bite angle of 92.77°. It is, therefore, difficult to draw conclusions on the effect of the ligand bite angle on branched selectivity, but when the branched substrate is used, the trend for branched selectivity generally increases with the size of the $P^{\wedge}P=S$ -metal ring with rare exceptions according to the following trend: five-membered ring < six-membered ring \approx seven-membered ring < eight-membered ring < nine-membered ring \approx dppf(S). We can conclude that the 9-membered rings and dppf(S) approach the optimum bite angle for branched selectivity. For these ligands that induce high branched selectivity, decreased temperature further increased selectivity for the branched product.

The most straightforward explanation for increased branched selectivity with larger rings is that larger ligands allow better “embracing” of the substrate by the phenyl groups on the donor atoms. This is expected to increase the preference of the allyl substituent for orientation of its more substituted terminus *cis* to S which places the electronically favored position for nucleophilic attack *trans* to P. The distortion of the η^3 -allyl is also expected to increase with increased bite angle [36].

The origin of branched regioselectivity has also been rationalized in terms of the relative amounts and stabilities of *syn* and *anti* isomers. It has been suggested that attack at a *syn* substituted position is disfavored while attack on an *anti* substituted allyl is favored at the more substituted position [4]. Generally, in a stoichiometric reaction, *syn* isomers have been shown to give (*E*)-linear product, while *anti* isomers give mainly branched and some (*Z*)-linear product. In catalytic reactions, the rate of *syn-anti*

isomerism relative to nucleophilic attack also influences selectivity. As suggested above for the orientation of the substituted terminus, an increased bite angle ligand will increase the relative preference for the *anti*-crotyl isomer. In the case of $P^{\wedge}P$ ligands, this effect has been proposed to explain both increased linear [45] and increased branched [4] selectivity with increased bite angle depending on the steric demands of the substrate. Since the analogous crotyl complexes of the $P^{\wedge}P=S$ allyl complexes studied here were not isolated, it is not clear if this rationalization would apply.

2.4. Memory effect

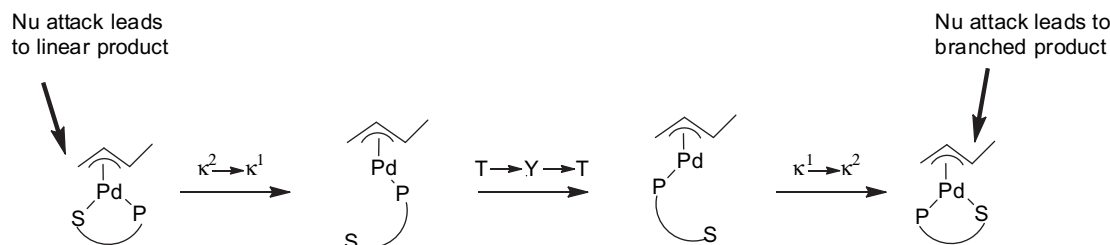
A regiochemical memory effect was observed for some of the $P^{\wedge}P=S$ donor ligands utilized. In previously observed allylic addition reactions this effect was found to be increased for certain monodentate phosphine ligands [30,32]. The memory effect refers to the observation that nucleophilic attack is more apt to occur at the position of the leaving group. In other words, for a given catalyst, the branched substrate yields a greater branched: linear ratio than the linear substrate. A common explanation of the memory effect phenomenon is that the equilibration rates of isomeric allylic palladium intermediates are slow relative to the rate of nucleophilic attack. Matched and mismatched pairs of palladium complexes derived from enantiotopic substituted allylic substrates with enantiopure ligands have been proposed to proceed through different mechanisms of allylic substitution resulting in a stereochemical memory effect [46].

The 3-buten-2-yl and crotyl carbonates are expected to add to palladium to give the same intermediates, but in some cases the memory of the position of the leaving group is maintained. Hayashi observed the formation of a neutral complex upon oxidative addition of an allylic acetate to a palladium complex of the large cone angle ligand MeO-MOP (Fig. 4) [32]. The leaving group leaves from the position *trans* to phosphorus so nucleophilic attack at the site *trans* to phosphorus results in retention of regiochemistry if allyl rearrangement is slow. Rhodium and iridium catalyzed allylic substitution reactions often display a regiochemical memory effect, but this has been attributed to the formation of an η^1 -allyl [23,24]. A regiochemical memory effect has also been observed for the alkylation of allylic benzoates with sodium dimethyl malonate catalyzed by $[Pd(\eta^3-C_3H_5)((S)-BINAP(S))][SbF_6]$ [10]. We propose a similar effect for our ligands, where nucleophilic attack will occur at the site originally occupied by the leaving group if allyl rearrangement or *cis-trans* isomerization is slow. We have previously reported studies of the relative rates of these processes occurring in complexes of several $P^{\wedge}P=S$ ligands [15].

This effect may also be related to the reaction rates observed. By microscopic reversibility, if nucleophilic attack occurs *trans* to phosphorus, then one expects the site of the leaving group to be oriented *trans* to phosphorus upon initial ionization of the allylic substrate. If no rearrangement occurs, one would expect branched substrate to yield branched product and linear substrate to yield linear product. It also follows that if orientation with the more substituted terminus *trans* to phosphorus is favored, then the linear substrate may react more slowly owing to the sterically unfavorable orientation of the bulky allylic terminus *cis* to phosphorus. The only ligands displaying no memory effect are xantphos(S) (i), DPEphos



Fig. 4. Hayashi's (R)-MeO-MOP ligand.



Scheme 2. A mechanism for *cis/trans* interconversion via ligand hemilability.

(S) (**h**) and diphos(S) (**c**). The former two ligands are among the most selective and form nine-membered ring with palladium which appears to be the optimum ring size for branched selectivity and may encourage fast allyl exchange relative to nucleophilic attack, thereby decreasing the contribution of memory effect with these ligands. Bite angle differences have been shown previously to affect the rate of allyl isomerization relative to nucleophilic attack [4]. Relative rates of hemilability may also contribute to the memory effect since hemilability can exchange the allylic positions *cis* and *trans* to the phosphorus donor. In fact, we reported [15] that xantphos(S) (**i**), which displays no memory effect, has a decreased barrier to hemilability relative to ligands **a**, **c**, **e**, and **g**.

One must recognize that *cis/trans* interconversion may also occur via a T–Y–T mechanism involving an η^1 -crotyl but retaining the κ^2 -P[∧]P=S, as shown in Scheme 3. It is rather difficult to delineate the relative rates of the interconversions via the paths in Schemes 2 and 3. Furthermore, although less likely, there is also the possibility of *cis/trans* interconversion via a bimolecular process involving pseudorotation of a five-coordinate intermediate formed by addition of another ligand.

Xantphos(S) (**i**) appears to approach the optimal bite angle that will allow for high regioselectivity for branched product coupled with high catalyst activity. A nine-membered ring appears to be optimal for branched selectivity since DPEphos(S) (**h**) is similar to xantphos(S) (**i**) in its selectivity despite its slightly smaller bite angle and increased flexibility when compared to other bisphosphine monosulfides. Dppf has a similar bite angle to DPEphos and its monosulfide results in similar regioselectivity when the branched substrate is used.

2.5. Hemilability and nonrigidity

The barrier to hemilability has been shown to decrease for ligands forming larger rings. Since those ligands also allow for increased branched selectivity, there may be a relationship between the ability of the ligands to rearrange via an η^1 intermediate and branched selectivity. Since this mechanism exchanges the *cis* and *trans* allylic positions, it may facilitate the reorientation of the substrate to the more favorable position with the substituted end *trans* to P. This may overcome the memory effect if hemilability occurs more rapidly than nucleophilic attack. We have shown previously that the large bite angle ligand xantphos(S) (**i**) has a low barrier to hemilability relative to the smaller bite angle P[∧]P=S

ligands studied [15]. This ligand allowed for high branched selectivity regardless of the substrate used, which is consistent with fast *cis/trans* exchange that eliminates the memory effect.

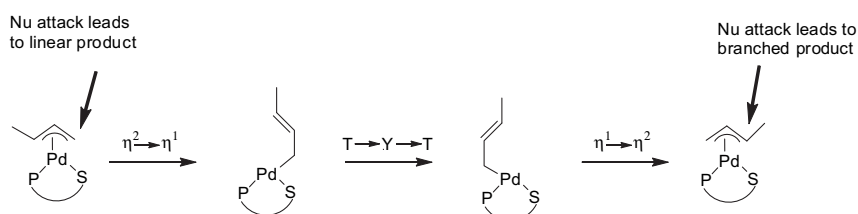
Another factor that may influence the selectivity of palladium-catalyzed allylic alkylations is ligand backbone rearrangement, but this does not directly effect which allylic terminus is *trans* to phosphorus, the position of nucleophilic attack. The complexes **1g–i** contain ligands with flexible backbones and are among the more active catalysts for palladium-catalyzed allylic alkylation. A less active catalyst is **1b** which contains a P[∧]P=S ligand that has a fixed backbone geometry. An increase in catalyst activity with increased backbone flexibility has been observed previously for palladium catalyzed allylic alkylations [45].

Complex **1d** also shows four ³¹P NMR resonances at low temperature (<–60 °C). At 45 °C the ³¹P NMR spectrum remains broad. It is probable that this complex forms two different isomers based on the position of the propyl backbone. An alternative is that the formation of the P[∧]P=S chelate is unfavorable with this ligand and a bimetallic species has formed. The exchange observed may be due to dissociation of the P=S moiety. This behavior has been observed previously with dppp(S) (**d**) [47,48]. Therefore, the fluxional processes that are available to each individual ligand may further influence branched selectivity, reaction rate and memory effect. One might note that flexible four-atom bridged bidentate ligands such as dppb, sometimes produce dimers; hence even greater number of species may need to be considered.

2.6. Structural aspects of xantphos(S) and DPEphos(S) complexes

As xantphos and DPEphos are particularly large bite angle ligands, X-ray crystallographic determinations of the monosulfide complexes were undertaken to assess the relative bite angles in the complexes with the increased chelate ring size. These metrical aspects were also of interest since these complexes were implicated in rapid crotyl isomeric intermediate interconversions. The crystallographic data are summarized in Table 3 and ORTEP views are shown in Figs. 5 and 6.

The flexibility of the chelate ring provided by the monosulfides decreases the bite angles relative to the parent large bite angle bisphosphines (Table 2). The preference for sulfur in P=S ligands to produce bonds to metals with angles ~90° yields rings with substantially different geometries relative to the bisphosphines. A



Scheme 3. A mechanism for *cis/trans* interconversion via an η^1 -crotyl.

Table 3
Crystallographic data for **1h** and **1i**.

	1h	1i
Color, shape	Colorless block	Colorless plate
Empirical formula	C ₃₉ H ₃₃ OFeP ₂ PdSSb	C ₄₃ H ₃₉ Cl ₂ F ₆ OP ₂ PdSSb
Formula weight	953.84	1078.83
Radiation/Å	Mo Kα (monochr.)	Mo Kα (monochr.)
<i>T</i> /K	173	173
Crystal system	Monoclinic	Monoclinic
Space group	<i>P</i> 2 ₁ / <i>n</i> (No. 14)	<i>C</i> c (No. 9)
Unit cell dimensions		
<i>a</i> /Å	13.5020(4)	9.2421(2)
<i>b</i> /Å	16.0393(4)	25.0472(7)
<i>c</i> /Å	17.3279(4)	18.4197(5)
β/deg	96.859(2)	91.567(2)
<i>V</i> /Å ³	3725.7(2)	4262.4(2)
<i>Z</i>	4	4
<i>D</i> _{calc} /g cm ⁻³	1.700	1.681
μ/cm ⁻¹ (Mo Kα)	14.10	13.64
Crystal size/mm	0.12 × 0.12 × 0.17	0.02 × 0.12 × 0.12
Total reflections, unique reflections	15792, 8843	8513, 6502
<i>R</i> _{int}	0.031	0.025
No. Obs (<i>I</i> > 3σ(<i>I</i>))	5697	5299
Parameters, constraints	464, 0	516, 0
<i>R</i> ^a , <i>R</i> _w ^b , GOF	0.030, 0.032, 1.08	0.031, 0.032, 1.15
resid. density/e Å ⁻³	-0.53 < 0.51	-0.51 < 0.46

^a $R = \sum ||F_o| - |F_c|| / \sum |F_o|$, for all $I > 3\sigma(I)$.

^b $R_w = [\sum [w(|F_o| - |F_c|)^2] / \sum [w(F_o)^2]]^{1/2}$.

striking difference offered by the backbone flexibility in the DPEphos(S) is that the backbone phenyls are nearly orthogonal; whereas they are constrained to be nearly parallel in the xantphos(S) complex.

The xantphos(S) ring system allows several conformational isomers and this provides the opportunity to vary the bite angle substantially. This is particularly notable in Table 2 when comparing the allylpalladium and COD rhodium complexes where the bite angles differ by ~10°. An ORTEP view of the previously published rhodium complex is provided in Fig. 7 to illustrate the conformational differences [15]. Note that in the rhodium complex the ligand tends to fold so that the backbone is near the metal; whereas in the palladium complex the backbone is remote from the metal.

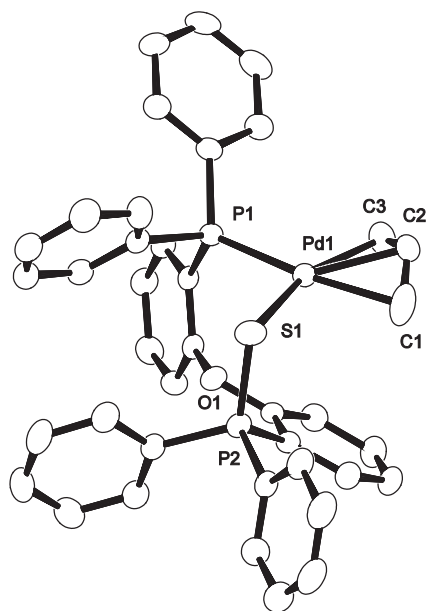


Fig. 5. An ORTEP view of the cation in **1h** with 50% probability ellipsoids. The P1–Pd–S angle is 99.23(3)° and the Pd–S–P2 angle is 105.12(4)°.

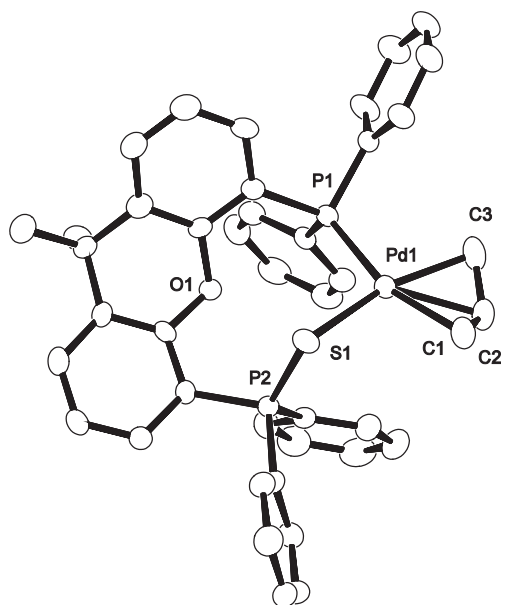


Fig. 6. An ORTEP view of the cation in **1i** with 50% probability ellipsoids. The P1–Pd–S angle is 102.59(5)° and the Pd–S–P2 angle is 107.86(6)°.

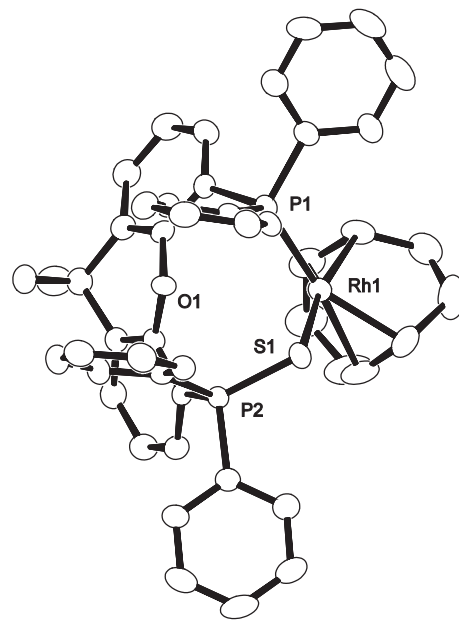


Fig. 7. An ORTEP view of the cation in [CODRh(Xantphos(S))][SbF₆] (DOBPUG) [15] with 50% probability ellipsoids. The P1–Pd–S angle is 92.99(4)° and the Pd–S–P2 angle is 108.47(5)°.

3. Conclusions

[Pd(η³-C₃H₅)(P[∧]P=S)][SbF₆] complexes have been shown to catalyze the allylic alkylation of carbonates with sodium dimethyl malonate with unusually high selectivity for addition to the substituted allylic terminus. P[∧]P=S ligands forming larger rings gave increased branched selectivity and furthermore, ligand backbone flexibility increased the rate of the reaction. There was also a significant memory effect observed with a number of P[∧]P=S ligands. Low temperatures increased the regioselectivity and the memory effect for the reaction. While the effect of bite angle is most likely the result of better embracing of the substrate, the

increased rate of hemilability may increase the rate of allyl equilibration, and decrease contributions from the memory effect by allowing more rapid *cis*–*trans* exchange. A difference in linear and branched substrate reactivity was also observed. Considering the increased interest in $P^{\wedge}S$ ligands for asymmetric allylic alkylation [43,49–56], the ability to tune ligands for high branched selectivity is a crucial aspect of developing highly selective catalysts for enantiopure branched products.

4. Experimental

4.1. General methods

All synthetic manipulations were performed under a nitrogen atmosphere using standard Schlenk techniques. CH_2Cl_2 was dried by distillation over CaH_2 and THF was dried by distillation over sodium and benzophenone. $[\text{Pd}(\eta^3\text{-C}_3\text{H}_5)\text{Cl}]_2$ [56], complexes **1a** [38], **1b** [11], **1c** [15], **1e** [10], **1f** [11], **1g** [15], and **1i** [15], were prepared by published methods. The previously known $P^{\wedge}P=S$ ligands **a** [57], **b** [11], **c** [58], **d** [58], **e** [10], **f** [11], **g** [59], and **i** [15], were prepared in analogy to the published method [41] and characterization data were in accord with those previously reported. Pentane and diethyl ether were used as received. NMR spectra were recorded on Bruker 400 or 500 MHz instruments and the chemical shifts reported in ppm relative to TMS via reference to solvent resonances for ^1H and ^{13}C spectra. The ^{31}P spectra were indirectly referenced to phosphoric acid via the lock frequency and Ξ values.

4.2. General procedure for preparation of $[\text{Pd}(\eta^3\text{-C}_3\text{H}_5)(P^{\wedge}P=S)][\text{SbF}_6]$ (**1**)

$[\text{Pd}(\eta^3\text{-C}_3\text{H}_5)\text{Cl}]_2$ (36.6 mg, 0.1 mmol) was dissolved in CH_2Cl_2 and one equivalent (0.2 mmol) of the appropriate $P^{\wedge}P=S$ ligand was added to the solution. NaSbF_6 (51.7 mg, 0.2 mmol) was then added and the mixture was stirred for 6 h at room temperature. The solution was filtered through Celite and the solvent removed by rotary evaporation. The compounds were crystallized from concentrated CH_2Cl_2 solutions layered with ether or pentane.

4.2.1. $[\text{Pd}(\eta^3\text{-C}_3\text{H}_5)(\text{dppp}(S))][\text{SbF}_6]$ (**1d**)

Yield: 62%. Exists as two isomers in a 5:1 ratio at -80°C ^1H NMR (500 MHz, CD_2Cl_2 , 0°C) δ : 7.81 (4H, m, Ph-*H*); 7.65 (2H, m, Ph-*H*); 7.41 (14H, m, Ph-*H*); 5.52 (1H, m, allyl-*H*, central, $^3J_{\text{HH}} = 7.6, 7.7, 12.6, 13.9$ Hz); 4.54 (1H, dd, allyl-*H*, *trans* to *P*, *syn*, $^3J_{\text{HH}} = 7.6$ Hz, $J_{\text{PH}} = 6.7$ Hz); 3.42 (1H, dd, allyl-*H*, *trans* to *P*, *anti*, $^3J_{\text{HH}} = 12.8$ Hz, $J_{\text{PH}} = 11.5$ Hz); 3.83 (1H, br, allyl-*H*, *cis* to *P*, *syn*); 3.00 (2H, m, CH_2); 2.89 (2H, m, CH_2); 2.73 (1H, br, allyl-*H*, *cis* to *P*, *anti*); 1.95 (2H, m, CH_2). ^{31}P NMR (162 MHz, CD_2Cl_2 , 0°C) δ : 42.8, br; 14.5 br. ^{31}P NMR (162 MHz, CD_2Cl_2 , -80°C) Major Isomer δ : 42.8; 13.2. Minor Isomer δ : 41.2 20.7. ^{13}C NMR (126 MHz, CD_2Cl_2) δ : 133.4 (d, Ph-C, $J_{\text{PC}} = 2.8$ Hz); 133.2–132.6 (br, Ph-C); 131.5 (d, Ph-C, $J_{\text{PC}} = 10.4$ Hz); 129.8 (d, Ph-C, $J_{\text{PC}} = 12.5$ Hz); 129.6 (d, Ph-C, $J_{\text{PC}} = 10.0$ Hz); 120.1 (1C, br, allyl- CH); 80.0 (1C, d, allyl- CH_2 , *trans* to *P*, $J_{\text{PC}} = 30.5$ Hz); 64.7 (1C, br, allyl- CH_2 , *cis* to *P*); 31.3 (1C, d, PCH_2 , $^1J_{\text{PC}} = 52.0$ Hz); 26.6 (1C, d, PCH_2 , $^1J_{\text{PC}} = 26.0$ Hz); 17.6 (1C, d, CH_2 , $^2J_{\text{PC}} = 4.1$ Hz). Anal. Calcd. for $\text{C}_{30}\text{H}_{31}\text{F}_6\text{P}_2\text{Pd}_1\text{S}_1\text{Sb}_1 \cdot 0.5\text{C}_5\text{H}_{12}$: C, 45.19; H, 4.32. Found: C, 45.26; H, 4.06.

4.2.2. $[\text{Pd}(\eta^3\text{-C}_3\text{H}_5)(\text{DPEphos}(S))][\text{SbF}_6]$ (**1h**)

Yield: 82%. Exists as two isomers in 3:2 ratio at 0°C ^1H NMR (400 MHz, CD_2Cl_2 , -20°C) Both isomers δ : 7.76–6.81 (56H, m, aromatic-*H*). Major isomer δ : 5.52 (1H, dddd, allyl-*H*, central, $^3J_{\text{HH}} = 6.5$ Hz, 7.1 Hz, 12.5 Hz, 13.5 Hz); 4.56 (1H, allyl-*H*, *trans* to *P*, *syn*, ddd, $^4J_{\text{HH}} = 1.7$ Hz, $^3J_{\text{HH}} = 7.1$ Hz, $J_{\text{PH}} = 7.3$ Hz); 3.77 (1H, allyl-*H*, *cis* to *P*, *syn*, dd, $^4J_{\text{HH}} = 1.7$ Hz, $^3J_{\text{HH}} = 6.5$ Hz); 2.58 (1H, allyl-*H*,

cis to *P*, *anti*, d, $^3J_{\text{HH}} = 12.5$ Hz); 1.70 (1H, allyl-*H*, *trans* to *P*, *anti*, dd, $^3J_{\text{HH}} = 13.5$ Hz, $J_{\text{PH}} = 10.8$ Hz). Minor isomer δ : 4.28 (1H, allyl-*H*, *trans* to *P*, *syn*, ddd, $^4J_{\text{HH}} = 2.2$ Hz, $^3J_{\text{HH}} = 7.5$ Hz, $J_{\text{PH}} = 7.3$ Hz); 4.10 (1H, dddd, allyl-*H*, central, $^3J_{\text{HH}} = 7.0$ Hz, 7.5 Hz, 12.6 Hz, 13.8 Hz); 3.94 (1H, allyl-*H*, *cis* to *P*, *syn*, dd, $^4J_{\text{HH}} = 2.2$ Hz, $^3J_{\text{HH}} = 7.0$ Hz); 3.53 (1H, allyl-*H*, *trans* to *P*, *anti*, dd, $^3J_{\text{HH}} = 13.8$ Hz, $J_{\text{PH}} = 9.3$ Hz); 2.65 (1H, allyl-*H*, *cis* to *P*, *anti*, d, $^3J_{\text{HH}} = 12.6$ Hz). ^{31}P NMR (162 MHz, CD_2Cl_2 , -20°C) Major isomer δ : 39.8, 11.9. Minor isomer δ : 40.2, 14.7. Anal. Calcd for $\text{C}_{39}\text{H}_{33}\text{O}_1\text{F}_6\text{P}_2\text{Pd}_1\text{S}_1\text{Sb}_1 \cdot \text{H}_2\text{O}$: C, 48.20; H, 3.63. Found: C, 48.38; H, 3.55.

4.3. Preparation of a new $P^{\wedge}P=S$ Ligand, DPEphos(S) (**h**)

This preparation followed the general procedure used for all of the monosulfides. The bisphosphine (2.5 mmol) was dissolved in THF, and 0.8 equivalent of sulfur (64.1 mg, 2.00 mmol) was added. The mixture was stirred until all of the sulfur dissolved and then the THF was removed by rotary evaporation. The resulting mixture of the bisphosphine, the bisphosphine monosulfide, and the bisphosphine disulfide was separated by column chromatography (silica gel, CH_2Cl_2 /hexane mixture). DPEphos(S) (**h**) ^1H NMR (500 MHz, CDCl_3) δ : 8.27 (1H, m, aromatic-*H*); 7.87–7.01 (22H, m, aromatic-*H*); 6.98 (1H, m, aromatic-*H*); 6.89 (1H, m, aromatic-*H*); 6.75 (1H, m, aromatic-*H*); 6.55 (1H, m, aromatic-*H*); 6.01 (1H, m, aromatic-*H*). ^{31}P NMR (162 MHz, CDCl_3) δ : 41.9 ($P=S$); -17.4 ($P(\text{III})$). Anal. Calcd for $\text{C}_{36}\text{H}_{28}\text{O}_1\text{P}_2\text{S}_1$: C, 75.78; H, 4.95. Found: C, 75.51; H, 4.95.

4.4. Catalysis studies

The data for Table 1 were obtained using the following general procedure. A 2.5% catalyst loading using (0.00525) mmol of complex **1a–h** was added to a flame-dried flask under nitrogen and then dissolved in 2 mL THF. The crotyl or butenyl substrate, 30.3 mg (0.210 mmol), was added and the temperature adjusted. A 50% excess of a stock THF solution of sodium dimethyl malonate that had been prepared from sodium hydride and a 3% excess of dimethyl malonate was added to the mixture (0.315 mmol, 1 mL). After the required time (1 h or 20 h), pentane was added to the reaction mixture and then the resulting mixture filtered through Celite. The products were isolated after evaporation of the solvent and the mixture analyzed by ^1H NMR.

4.5. Structure determination and refinement

Data were collected on a Nonius KappaCCD (Mo $K\alpha$ radiation) diffractometer at -100°C and were not specifically corrected for absorption other than the inherent corrections provided by Scalepack [60]. The structures were solved by direct methods (SIR92) [61] and refined on F for all reflections [62]. Non-hydrogen atoms were refined with anisotropic displacement parameters. Hydrogen atoms were included at calculated positions. Relevant crystal and data parameters are presented in Table 3. Atomic coordinates were deposited with the Cambridge Crystallographic Data Centre.

4.5.1. $[\text{Pd}(\eta^3\text{-C}_3\text{H}_5)(\text{DPEphos}(S))][\text{SbF}_6]$ (**1h**)

Crystals were obtained by slow diffusion of pentane into a methylene chloride solution of **1h**. The complex crystallized in the monoclinic space group $P2_1/n$. The cation showed a 2:1 disorder in the orientation of the allyl as indicated by common positions for the terminal carbons of the allyl and the central carbon distributed above and below the S–Pd–P plane. Owing to the disorder the C1–C2 and C2–C3 bond lengths are not reliable; however the Pd–C1 and Pd–C3 bond lengths of 2.184(4) and 2.133(3) show the expected relative lengthening *trans* to *P*.

4.5.2. $[Pd(\eta^3-C_3H_5)(Xantphos(S))][SbF_6]$ (**1i**)

Crystals were obtained by slow diffusion of pentane into a methylene chloride solution of **1i**. The complex crystallized in the monoclinic space group *Cc* with one molecule of methylene chloride in the asymmetric unit. The cation showed an 85:15 disorder in the orientation of the allyl as indicated by common positions for the terminal carbons of the allyl and the central carbon distributed above and below the S–Pd–P plane. Owing to the disorder the C1–C2 and C2–C3 bond lengths are not reliable; however the Pd–C1 and Pd–C3 bond lengths of 2.199(6) Å and 2.113(6) Å show the expected relative lengthening *trans* to P.

4.5.3. $[CODRh(Xantphos(S))][SbF_6]$

The structure of $[CODRh(Xantphos(S))][SbF_6]$ was published previously [15] and is available in the Cambridge Crystallographic Data Base under ref code DOBPUG.

Acknowledgements

We thank the donors of the Petroleum Research Fund administered by the American Chemical Society for support of our work (PRF#43212). We thank Jonathan Parr for helpful comments.

Appendix A. Supplementary data

CCDC No. 788058 and 788059 contain the supplementary crystallographic data for compounds **1h** and **1i** of this paper. These data can be obtained free of charge from The Cambridge Crystallographic Data Centre via www.ccdc.cam.ac.uk/data_request/cif.

References

- [1] E.N. Jacobsen, A. Pfaltz, H. Yamamoto (Eds.), *Comprehensive Asymmetric Catalysis*, vols. 1–3, Springer, Berlin, 1999.
- [2] B.M. Trost, D.L. Vanvraken, C. Bingel, *J. Am. Chem. Soc.* 114 (1992) 9327.
- [3] P. van Leeuwen, P.C.J. Kamer, J.N.H. Reek, P. Dierkes, *Chem. Rev.* 100 (2000) 2741.
- [4] R.J. van Haaren, H. Oevering, B.B. Coussens, G.P.F. van Strijdonck, J.N.H. Reek, P.C.J. Kamer, P. van Leeuwen, *Eur. J. Inorg. Chem.* (1999) 1237.
- [5] B.M. Trost, D.L. Vanvraken, *Chem. Rev.* 96 (1996) 395.
- [6] B.M. Trost, M.L. Crawley, *Chem. Rev.* 103 (2003) 2921.
- [7] J.W. Faller, B.J. Grimmond, D.G. D'Alliessi, *J. Am. Chem. Soc.* 123 (2001) 2525.
- [8] G. Helmchen, A. Pfaltz, *Acc. Chem. Res.* 33 (2000) 336.
- [9] J. Sprinz, M. Kiefer, G. Helmchen, G. Huttner, O. Walter, L. Zsolnai, M. Reggelin, *Tetrahedron Lett.* 35 (1994) 1523.
- [10] J.W. Faller, J.C. Wilt, J. Parr, *Org. Lett.* 6 (2004) 1301.
- [11] J.W. Faller, J.C. Wilt, *Organometallics* 24 (2005) 5076.
- [12] J.W. Faller, N.J. Zhang, K.J. Chase, W.K. Musker, A.R. Amaro, C.M. Semko, *J. Org. Chem.* 468 (1994) 175.
- [13] P. Braunstein, F. Naud, *Angew. Chem. Int. Ed.* 40 (2001) 680.
- [14] C.W. Rogers, M.O. Wolf, *Chem. Commun.* (1999) 2297.
- [15] J.W. Faller, S.C. Milheiro, J. Parr, *J. Organomet. Chem.* 693 (2008) 1478.
- [16] G.C. Lloyd-Jones, A. Pfaltz, *Angew. Chem. Intl. Ed.* 34 (1995) 462.
- [17] B.M. Trost, K. Dogra, *Org. Lett.* 9 (2007) 861.
- [18] S.W. Krska, D.L. Hughes, R.A. Reamer, D.J. Mathre, M. Palucki, N. Yasuda, Y. Sun, B.M. Trost, *Pure Appl. Chem.* 76 (2004) 625.
- [19] B.M. Trost, M.H. Hung, *J. Am. Chem. Soc.* 106 (1984) 6837.
- [20] P.A. Evans, J.D. Nelson, *J. Am. Chem. Soc.* 120 (1998) 5581.
- [21] P.A. Evans, J.D. Nelson, *Tetrahedron Lett.* 39 (1998) 1725.
- [22] P.A. Evans, L.J. Kennedy, *Org. Lett.* 2 (2000) 2213.
- [23] P.A. Evans, L.J. Kennedy, *J. Am. Chem. Soc.* 123 (2001) 1234.
- [24] G. Helmchen, A. Dahnz, P. Dubon, M. Schelwies, R. Weihofen, *Chem. Commun.* (2007) 675.
- [25] D. Polet, A. Alexakis, K. Tissot-Croset, C. Corminboeuf, K. Ditrach, *Chem. Eur. J.* 12 (2006) 3596.
- [26] B. Bartels, G. Helmchen, *Chem. Commun.* (1999) 741.
- [27] R. Takeuchi, M. Kashio, *J. Am. Chem. Soc.* 120 (1998) 8647.
- [28] J.P. Janssen, G. Helmchen, *Tetrahedron Lett.* 38 (1997) 8025.
- [29] B. Akermarck, K. Zetterberg, S. Hansson, B. Krakenberger, A. Vitagliano, *J. Org. Chem.* 335 (1987) 133.
- [30] J.W. Faller, N. Sarantopoulos, *Organometallics* 23 (2004) 2179.
- [31] R.J. van Haaren, P.H. Keeven, L.A. van der Veen, K. Goubitz, G.P.F. van Strijdonck, H. Oevering, J.N.H. Reek, P.C.J. Kamer, P. van Leeuwen, *Inorg. Chim. Acta* 327 (2002) 108.
- [32] T. Hayashi, M. Kawatsura, Y. Uozumi, *Chem. Commun.* (1997) 561.
- [33] R. Pretot, A. Pfaltz, *Angew. Chem. Int. Ed.* 37 (1998) 323.
- [34] O. Pamies, M. Dieguez, C. Claver, *J. Am. Chem. Soc.* 127 (2005) 3646.
- [35] V. Branchadell, M. Moreno-Manas, F. Pajuelo, R. Pleixats, *Organometallics* 18 (1999) 4934.
- [36] R.J. van Haaren, K. Goubitz, J. Fraanje, G.P.F. van Strijdonck, H. Oevering, B. Coussens, J.N.H. Reek, P.C.J. Kamer, P. van Leeuwen, *Inorg. Chem.* 40 (2001) 3363.
- [37] P. Dierkes, P. van Leeuwen, *J. Chem. Soc. Dalton Trans.* (1999) 1519.
- [38] O. Piechaczyk, M. Doux, L. Ricard, P. le Floch, *Organometallics* 24 (2005) 1204.
- [39] T.Y.H. Wong, S.J. Rettig, B.R. James, *Inorg. Chem.* 38 (1999) 2143.
- [40] E.I. Matrosova, Z.A. Starikova, D.I. Lobanov, I.M. Aladzheva, O.V. Bykhovskaya, T.A. Mastryukova, *Russ. Chem. Bull.* 49 (2000) 1116.
- [41] J.W. Faller, P.P. Fontaine, *J. Organomet. Chem.* 692 (2007) 976.
- [42] J.W. Faller, J.C. Wilt, *J. Organomet. Chem.* 691 (2006) 2207.
- [43] J.W. Faller, J.C. Wilt, *Org. Lett.* 7 (2005) 633.
- [44] R. Broussier, E. Bentabet, M. Laly, P. Richard, L.G. Kuz'mina, P. Serp, N. Wheatley, P. Kalck, B. Gautheron, *J. Org. Chem.* 613 (2000) 77.
- [45] R.J. van Haaren, G.P.F. van Strijdonck, H. Oevering, J.N.H. Reek, P.C.J. Kamer, P. van Leeuwen, *Eur. J. Inorg. Chem.* (2001) 837.
- [46] B.J. Lussem, H.J. Gais, *J. Org. Chem.* 69 (2004) 4041.
- [47] D.K. Dutta, P. Chutia, J.D. Woollins, A.M.Z. Slawin, *Inorg. Chim. Acta* 359 (2006) 877.
- [48] A. Lofu, P. Mastrorilli, C.F. Nobile, G.P. Suranna, P. Frediani, J. Iggo, *Eur. J. Inorg. Chem.* (2006) 2268.
- [49] F.L. Lam, F.Y. Kwong, A.S.C. Chan, *Chem. Commun.* 46 (2010) 4649.
- [50] S. Gladioli, S. Medici, G. Pirri, S. Pulacchini, D. Fabbri, *Can. J. Chem.* 79 (2001) 670.
- [51] E. Guimet, M. Dieguez, A. Ruiz, C. Claver, *Tetrahedron: Asymmetry* 16 (2005) 959.
- [52] O. Pamies, G.P.F. van Strijdonck, M. Dieguez, S. Deerenberg, G. Net, A. Ruiz, C. Claver, P.C.J. Kamer, P. van Leeuwen, *J. Org. Chem.* 66 (2001) 8867.
- [53] H. Pellissier, *Tetrahedron* 63 (2007) 1297.
- [54] W. Zhang, M. Shi, *Tetrahedron: Asymmetry* 15 (2004) 3467.
- [55] E. Martin, M. Dieguez, *C.R. Chim.* 10 (2007) 188.
- [56] T. Hayashi, A. Yamamoto, Y. Ito, E. Nishioka, H. Miura, K. Yanagi, *J. Am. Chem. Soc.* 111 (1989) 6301.
- [57] S.O. Grim, E.D. Walton, *Inorg. Chem.* 19 (1980) 1982.
- [58] E.I. Matrosova, Z.A. Starikova, A.I. Yanovsky, D.I. Lobanov, I.M. Aladzheva, O.V. Bykhovskaya, Y.T. Struchkov, T.A. Mastryukova, M.I. Kabachnik, *J. Organomet. Chem.* 535 (1997) 121.
- [59] G. Pilloni, B. Longato, G. Bandoli, *Inorg. Chim. Acta* 277 (1998) 163.
- [60] W. Minor, Z. Otwinowski (Eds.), *HKL2000 (Denzo-SMN) software package*. "Processing of X-ray Diffraction Data Collected in Oscillation Mode", *Methods in Enzymology, Macromolecular Crystallography*, Academic Press, New York, 1997.
- [61] A. Altomare, G. Casciaro, C. Giacovazzo, A. Guagliardi, M. Burla, G. Polidori, M. Camalli, *J. Appl. Crystallogr.* 27 (1994) 435.
- [62] Texsan, *TEXSAN for Windows version 1.06: Crystal Structure Analysis Package*, Molecular Structure Corporation (1997–9) (1999).